AGU PUBLICATIONS

Geophysical Research Letters

RESEARCH LETTER
10.1002/2016GL068210

Key Points:
- Sediment composition leaves a distinct signature on delta channel network complexity
- As deltas evolve and reach steady state, complexity also achieves steady state
- A TopoDynamic complexity space offers potential for process inference and delta classification

Correspondence to:
A. Tejedor,
alej.tejedor@gmail.com

Citation:
Tejedor, A., A. Longjas, R. Caldwell, D. A. Edmonds, I. Zaliapin, and E. Foufoula-Georgiou (2016), Quantifying the signature of sediment composition on the topologic and dynamic complexity of river delta channel networks and inferences toward delta classification, *Geophys. Res. Lett.*, *43*, doi:10.1002/2016GL068210.

Received 10 FEB 2016
Accepted 11 MAR 2016
Accepted article online 18 MAR 2016

Quantifying the signature of sediment composition on the topologic and dynamic complexity of river delta channel networks and inferences toward delta classification

Alejandro Tejedor[1], Anthony Longjas[1], Rebecca Caldwell[2], Douglas A. Edmonds[2], Ilya Zaliapin[3], and Efi Foufoula-Georgiou[1,4]

[1]National Center for Earth-surface Dynamics and St. Anthony Falls Laboratory, University of Minnesota, Twin Cities, Minneapolis, Minnesota, USA, [2]Department of Geological Sciences and Center for Geospatial Data Analysis, Indiana University, Bloomington, Bloomington, Indiana, USA, [3]Department of Mathematics and Statistics, University of Nevada, Reno, Reno, Nevada, USA, [4]Department of Civil, Environmental, and Geo- Engineering, University of Minnesota, Twin Cities, Minneapolis, Minnesota, USA

Abstract Deltas contain complex self-organizing channel networks that nourish the surface with sediment and nutrients. Developing a quantitative understanding of how controlling physical mechanisms of delta formation relate to the channel networks they imprint on the landscape remains an open problem, hindering further progress on quantitative delta classification and understanding process from form. Here we isolate the effect of sediment composition on network structure by analyzing Delft3D river-dominated deltas within the recently introduced graph-theoretic framework for quantifying complexity of delta channel networks. We demonstrate that deltas with coarser incoming sediment tend to be more complex topologically (increased number of pathways) but simpler dynamically (reduced flux exchange between subnetworks) and that once a morphodynamic steady state is reached, complexity also achieves a steady state. By positioning simulated deltas on the so-called TopoDynamic complexity space and comparing with field deltas, we propose a quantitative framework for exploring complexity toward systematic inference and classification.

1. Introduction

River deltas are complex systems that exhibit a large variability in their morphology as a consequence of the physical processes that shape them, e.g., external forcings [*Wright and Coleman*, 1973; *Galloway*, 1975] and sediment composition [*Orton and Reading*, 1993; *Edmonds and Slingerland*, 2010]. Understanding and quantifying the patterns imprinted on the landscape as a function of the physical processes that created them will enable us to infer processes from observed imagery and also pave the way to a quantitative approach to delta classification, which is currently lacking.

Galloway [1975] introduced a ternary diagram to classify deltas, showing how the balance of upstream (fluvial) and downstream (waves and tides) forcings dictates the delta form, depicted most distinctively in the coastline morphology. Thus, river-dominated deltas tend to form lobate shapes that extend seaward, wave-dominated deltas are characterized by curved shorelines and beach ridges, and tide-dominated deltas contain many stretched islands perpendicular to the shoreline. However, the power of discrimination of this first-order classification is limited, since deltas with the same forcing can exhibit broad variability in delta morphology [e.g., *Caldwell and Edmonds*, 2014], implying that additional parameters can have a significant control. Recognizing this, *Orton and Reading* [1993] incorporated into the Galloway scheme a fourth dimension to account for the prevailing size of the sediment delivered to the delta, where four sediment categories were considered: mixed mud and silt, fine sand, gravelly sand, and gravel.

While the above classification schemes are insightful, they are not quantitative, reducing their predictive power. Some efforts to introduce quantitative tools to describe and compare delta morphologies have emerged in recent years. Specifically, metrics have been proposed for river-dominated (bifurcation-driven and minimally affected by waves and tides) [*Edmonds et al.*, 2011], tide-dominated [*Passalacqua et al.*, 2013] (and for tidal flats) [*Fagherazzi et al.*, 1999; *Rinaldo et al.*, 1999a, 1999b], and wave-dominated [*Jerolmack and Swenson*, 2007; *Nienhuis et al.*, 2015] deltas. The seminal work of *Smart and Moruzzi* [1971]

proposed the use of graph theory for studying the intricate structure of delta channel networks with the hope to relate the dominant processes and mechanisms acting on deltas to the channel morphology they imprint on the landscape. This preliminary study precipitated a new body of research focusing on the study of delta channel networks as connected graphs [*Morisawa*, 1985; *Marra et al*., 2014; *Hiatt and Passalacqua*, 2015; *Tejedor et al*., 2015a, 2015b]. In particular, *Tejedor et al*. [2015a] presented a rigorous mathematical framework for studying delta channel networks as directed graphs and showed that by algebraic operations on the adjacency matrix, several topologic and dynamic properties of deltas can be computed. Specifically, a delta channel network was decomposed into its apex-to-outlet subnetworks (hereafter also referred to as subnetworks), each consisting of the set of channels that connect the apex with each of the shoreline outlets. Then, a suite of metrics that capture the topologic complexity (connectivity structure of channel pathways) and dynamic complexity (exchange of fluxes among delta subnetworks) was introduced in *Tejedor et al*. [2015b] together with the so-called TopoDynamic complexity space where each delta can be uniquely positioned.

The ultimate goal is to apply these metrics to field-scale deltas to infer process from form and pave the way to classification. Indeed, *Tejedor et al*. [2015b] positioned seven deltas of variable origin, age, and structure on the TopoDynamic space and reported preliminary assessments. Further progress, however, requires a systematic examination of deltas with known underlying processes to start teasing apart the effect of specific controlling variables and mechanisms on the resulting delta channel network complexity. Toward this goal, physical experiments [*Hoyal and Sheets*, 2009; *Wolinsky et al*., 2010; *Straub et al*., 2015] and numerical simulations [*Edmonds and Slingerland*, 2010; *Geleynse et al*., 2011; *Caldwell and Edmonds*, 2014; *Liang et al*., 2015a, 2015b] offer "playgrounds" within which to explore systematically the effect of the physics on the morphology of delta channel networks. For example, using a high-resolution morphodynamic model, Delft3D, it has been shown that changing the sediment properties alone such as incoming sediment cohesion [*Edmonds and Slingerland*, 2010], grain size distribution [*Caldwell and Edmonds*, 2014], and initial subsurface cohesion [*Geleynse et al*., 2011] can cause a dramatic change in river-dominated delta morphologies (channel network, coastline, and planform morphology). Specifically, increasing the median grain size (D_{50}), dominant grain size (D_{84}), and decreasing the percent cohesive sediment results in a transition from elongated deltas with a few channels to semicircular deltas with many channels. Sediment composition also changes the morphodynamic processes operating on deltas with coarse-grained, noncohesive deltas having many channels dominated by avulsion while finer-grained cohesive deltas having fewer channels dominated by levee growth and channel extension [*Caldwell and Edmonds*, 2014].

Capitalizing on the quantitative framework proposed by *Tejedor et al*. [2015a, 2015b] together with the exploratory capability offered by numerical models, we seek to quantify the signature of a specific physical parameter, namely, the incoming sediment size (keeping all other variables fixed, e.g., no tidal and wave energy, no variability in incoming flow, and no vegetation) on the topologic and dynamic complexity of the emerging delta channel network. We show that river-dominated deltas built from coarser incoming sediment load exhibit channel networks that tend to be (1) more complex topologically, as reflected in increased channel loopiness (physically attributed to increased morphodynamic activity on the deltaic surface) and (2) less complex dynamically, as reflected by a higher degree of flux exchange between apex-to-outlet subnetworks (physically attributed to increased avulsion rates). We also show how complexity changes as a delta evolves reaching a statistical steady state and we discuss how the so-called TopoDynamic complexity space can be explored toward process inference and delta classification.

2. Methods

2.1. Delft3D Numerical Simulations

We use Delft3D to simulate the self-formed evolution of delta distributary networks. Delft3D is a physics-based morphodynamic model that has been validated for morphodynamics applications [e.g., *Lesser et al*., 2004] and germane to this paper it can create river deltas that resemble natural ones in terms of several statistical attributes [*Edmonds et al*., 2011]. We employ the depth-averaged version of Delft3D, which solves the unsteady shallow water equations in the horizontal dimension and assumes hydrostatic pressure in the vertical. Specifically, in this paper, we use model runs from *Caldwell and Edmonds* [2014] which simulate a sediment-laden river entering a standing body of water that is devoid of waves, tides, and buoyancy forces. The river has an upstream water discharge boundary condition (steady flow of $1000\,m^3\,s^{-1}$) and carries

sediment fluxes in equilibrium with the flow field. The downstream water surface boundary conditions are fixed at sea level. The flow field is coupled to the sediment transport equations [*van Rijn*, 1984a; 1984b] and bed surface equations so it dynamically evolves in response to sediment transport gradients.

The incoming sediment consists of grain sizes, D, lognormally distributed with a median size, D_{50}, and standard deviation $\sigma(\phi)$ (in ϕ space, where $\phi = -\log_2 D$). We note that cohesiveness (defined as the percent of sediment with grain size $D \leq D_c = 0.064$ mm) and dominant grain size (D_{84}) can be uniquely determined as a function of D_{50} and $\sigma(\phi)$ when the sediment size is lognormally distributed. Notice that other variables that can affect directly or indirectly the bulk cohesion of the system (e.g., vegetation, flow variability, and spatial heterogeneities from apex to shoreline) have not been considered here. Specifically, we compare six runs where the only difference is the median of the incoming grain size distributions D_{50}, while the standard deviation is fixed to $\sigma(\phi) = 1$. The distributions have median sizes of 0.01 mm, 0.05 mm, 0.1 mm, 0.25 mm, 0.5 mm, and 1 mm, respectively. These simulations are identical to runs B1a1, B1c1, B1e1, B1h1, B1m1, and B1o1 in Table 2 of *Caldwell and Edmonds* [2014], exploring the whole range of cohesiveness (from 0% to 100%) and values of dominant grain size from 0.014 to 1.896 mm. For more discussion on the morphodynamics of these deltaic simulations, see *Caldwell and Edmonds* [2014].

2.2. Channel Network Extraction and Analysis

The analysis conducted in this paper relies on spectral graph theory, which requires transforming each delta channel network into a graph. Graphs are mathematical objects composed of vertices and edges. For delta channel networks, the edges represent channels, and vertices correspond to the locations where one channel splits into new channels (bifurcation) or two or more channels merge into a single channel (junction). In preprocessing the gridded data produced by the simulations, we perform the following steps:

1. *Classify pixels as Land/Channels/Ocean*: First, we define a shoreline with the opening angle method [*Shaw et al*., 2008] on a binarized image where bed elevations below sea level were considered water and above sea level were considered land. We use an opening angle of 70°. All pixels not within the shoreline are defined as ocean. Within the enclosed shoreline, pixels are defined as channels if depth > 0.25 m, velocity $> 0.2\ \mathrm{m\,s^{-1}}$, and sediment transport rate $> 2.25 \times 10^{-5}\mathrm{m^3 s^{-1}}$. Everything else within the shoreline is defined as land.
2. *Eliminate disconnected channels*: From all the channel pixels, we only consider those ones that belong to channel pathways that eventually drain from the apex to the shoreline, removing isolated pixels and paths.
3. *Extract skeleton network*: We use an algorithm [*Lam et al*., 1992, page 879] to define the centerline of each channel, taking into account that channels can have a large range of variation in widths (from one pixel to several). From the resulting skeleton structure and flow directions, we define the vertices and edges that uniquely determine the directed graph corresponding to the delta channel network [e.g., see *Tejedor et al*., 2015a, Figure 7].
4. *Compute adjacency matrix*: All information about the network connectivity can be stored in a sparse matrix called *adjacency* matrix. The element of the matrix a_{ij} is different from zero if the vertex j is directly connected to downstream vertex i, and zero otherwise.
5. *Extract channel widths*: The width of channels measured directly downstream of each bifurcation is stored and used as a proxy for flux partition [see *Tejedor et al*., 2015a, section 2.2].

2.3. Metrics of Complexity

From the suite of topologic and dynamic complexity metrics proposed in *Tejedor et al*. [2015b], ranging from resistance distance to entropy-based measures, we employ here the two simplest and most intuitive metrics, namely: (1) for topologic complexity, we use the number of alternative paths of each apex-to-outlet subnetwork, which measures the degree of channel loopiness, and (2) for dynamic complexity, we use the Leakage Index, which captures the flux exchange among the subnetworks [see *Tejedor et al*., 2015b, Figure 1].

2.3.1. Topologic Complexity: Number of Alternative Paths (N_{ap})

The number of alternative paths (N_{ap}) corresponds to the intuitive notion of counting how many different ways a package of flux can travel from the apex to a given outlet at the shoreline. This metric is computed individually for each subnetwork i and its value depends on the number of loops and their relative arrangement within that subnetwork. For a delta with N subnetworks, the set of $N_{ap,i}$, $i = 1,2, \ldots, N$ values is computed

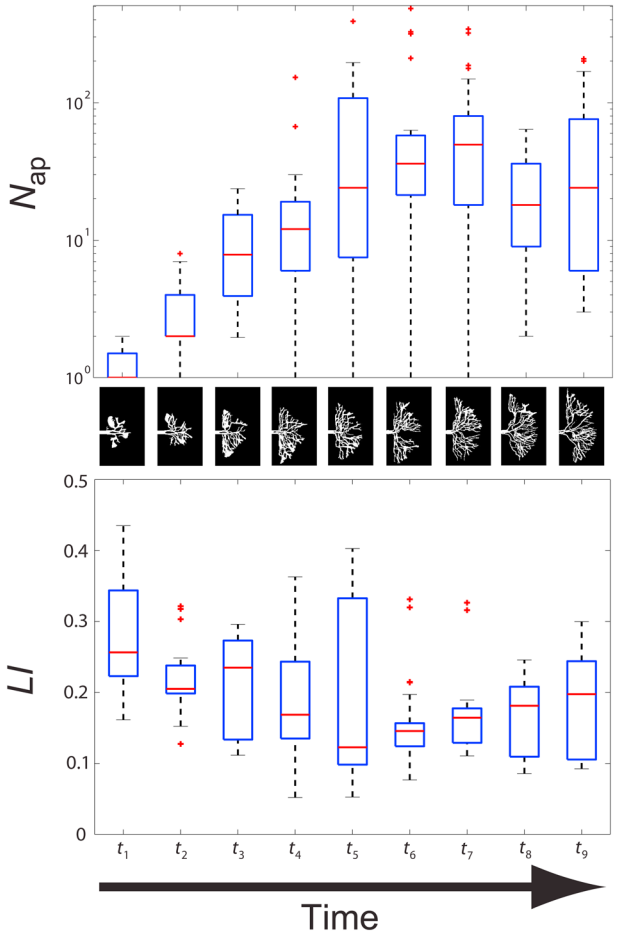

Figure 1. Delta evolution and complexity. For a Delft3D simulated delta with $D_{50} = 1.00$ mm (see text for details), the number of alternative paths (N_{ap}) increases and the Leakage Index (LI) decreases reaching an almost constant value when the delta has achieved a steady state, which occurs halfway through the total run time. The vertical boxplots extend between the $Q_1 = 25$th and $Q_3 = 75$th empirical quantiles of the distribution of the N_{ap} and LI values, respectively, computed for all the apex-to-outlet subnetworks, while the red line indicate the medians of these distributions. The whiskers extend between the minimal and maximal value within the interval $[Q_1 - 1.5 \times \text{IQR}, Q_3 + 1.5 \times \text{IQR}]$ with the interquartile range $\text{IQR} = Q_3 - Q_1$. The individual values outside of this interval are shown by red crosses.

representing the topologic complexity of the delta. Note that in the special case of a purely bifurcating delta, e.g., binary tree, all the subnetworks consist of single paths joining the apex to the shoreline outlets, having therefore $N_{ap} = 1$ for all subnetworks. Within the graph-theoretic framework, the number of alternative paths, for any subnetwork, can be computed via algebraic operations on the adjacency matrix [see *Tejedor et al.*, 2015b, section 3.1.1 and Appendix A for proof].

2.3.2. Dynamic Complexity: Leakage Index (*LI*)

Tejedor et al. [2015a, section 3.2] showed that the fluxes at every channel of the network at steady state can be computed via algebraic operations on the so-called weighted Laplacian matrix. This matrix is equivalent to a diffusivity operator on a graph, where the weights account for the flux partitioning at every bifurcation, here set equal to the relative widths of the channels downstream of each bifurcation. Notice that within this framework the computed steady state flux is conserved by definition, i.e., the flux entering the system through the apex is equal to the sum of the fluxes leaving the delta through its shoreline outlets. The conservation of flux also applies to all apex-to-outlet subnetworks in the steady state and takes into account the possible exchange of flux between subnetworks. This exchange of flux (e.g., leakage from subnetwork i to the rest of the delta) occurs at shared bifurcations at the border of the subnetwork i with other subnetworks wherein one of the downstream splitting channels still belongs to subnetwork i, whereas the other channel does not and therefore drains to an outlet different than that of subnetwork i. Hence, a metric that quantifies the proportion of flux that leaks out from each subnetwork to other subnetworks adds important new information, which encapsulates both the relative arrangement of the subnetworks within the delta network as a whole (something not captured by N_{ap}) and the network-wide distribution and dynamic partition of steady state fluxes.

We define the Leakage Index of a subnetwork i as the ratio $LI_i = F_i^{out}/F_i$, where F_i is the total flux, i.e., the sum of the steady state fluxes of all channels belonging to subnetwork i, and F_i^{out} is the sum of the fluxes leaking out from subnetwork i. The set of Leakage Index (LI_i) values for all subnetworks, $i = 1, 2, \ldots, N$, of the delta network captures the dynamic interaction among subnetworks and thus quantifies the dynamic complexity of the delta network as a whole [*Tejedor et al.*, 2015b, section 4.1]. The Leakage Index can vary in the interval [0,1), where an LI equal to zero implies a *sealed* subnetwork, i.e., all the flux that enters the subnetwork is drained to its own outlet, having no flux exchange with the rest of the system. On the other extreme, an LI value approaching one corresponds to a subnetwork that leaks out almost all its flux to the rest of the system delivering a minimal flux to its outlet.

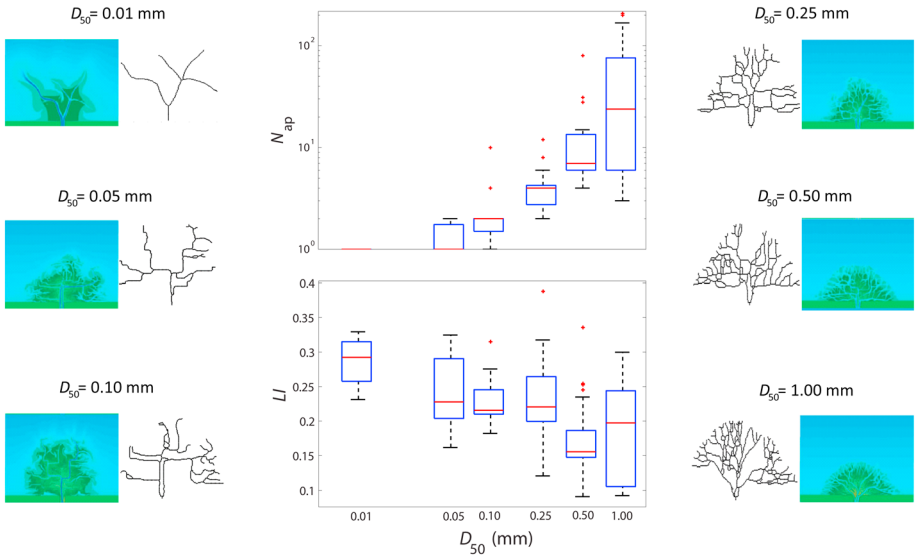

Figure 2. Effect of the median grain size (D_{50}) of incoming sediment on the delta channel network. Increasing D_{50} results in a transition from deltas with a few channels having low topologic complexity (as measured by the small number of alternative paths, N_{ap}) but high dynamic complexity (as measured by the high value of the Leakage Index, *LI*) to deltas with many loopy channels (of high topologic complexity but low dynamic complexity). See caption of Figure 1 for the definition of the vertical box plots and whiskers.

2.3.3. Topodynamic Complexity Space

Tejedor et al. [2015b] first introduced the so-called TopoDynamic complexity space where deltas can be projected and compared. The TopoDynamic complexity space is in general a multidimensional space with each dimension corresponding to a topologic or dynamic metric capturing attributes of delta complexity. In this paper, the TopoDynamic complexity space is defined using the number of alternative paths (topologic complexity) and Leakage Index (dynamic complexity) as dimensions. Notice that those two variables are not expected to be totally independent, since *LI* also carries information about the delta topology. However, it is not trivial to determine the type of this dependency as well as its strength, since the attributes of topology described by these two metrics are intrinsically different (i.e., N_{ap} is a property of each subnetwork independently of the rest of the delta, while *LI* depicts both the whole delta network topology that determines the steady state fluxes and the interaction among subnetworks).

3. Results and Discussion

3.1. Temporal Evolution

The questions as to (a) how the complexity of channel networks changes over time and (b) if this complexity reaches a stable value when a delta achieves a statistical steady state have not been studied before. One reason is the absence of long-term observations of evolving deltas. Here we use the modeled deltas to examine these questions. Figure 1 (middle) shows the temporal evolution of a Delft3D-simulated delta with a lognormal distribution of incoming sediment grain size characterized by $D_{50} = 1.0$ mm and $\sigma(\phi) = 1$ as captured at nine different instants of time. Visual inspection suggests that deltas exhibit morphologic changes as they evolve in time and experience avulsions and channel splitting and rejoining. Quantitatively, we document that during delta evolution the number of alternative paths (topologic complexity) increases and the Leakage Index (dynamic complexity) decreases, with both metrics reaching fairly constant values at a normalized time (time elapsed relative to total run time) of ~ 0.5 (see Figure 1 (top and bottom)). This suggests that deltas reach a steady state in terms of their complexity. This is consistent with a similar behavior observed in the metrics proposed by *Caldwell and Edmonds* [2014], namely, average topset gradient, number of channel mouths, and delta front rugosity. The fact that the complexity metrics stabilize at steady state is important to note as they give confidence in the steady state comparisons of delta patterns under different sediment properties discussed below.

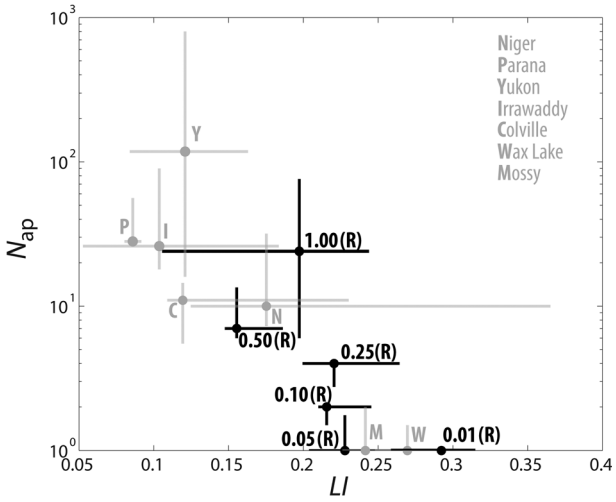

Figure 3. Two-dimensional TopoDynamic space of delta complexity. Combining the Number of alternative (N_{ap}) paths and Leakage Index (LI), we can map simulated deltas (black, labeled by D_{50} (R), where D_{50} is the median grain size of the incoming sediment, and R stands for river-dominated) in the TopoDynamic space according to their complexity. For river-dominated simulated deltas, as the grain size increases (D_{50} ranging from 0.01 to 1.00 mm), the topologic complexity (N_{ap}) increases and dynamic complexity (LI) decreases. Seven field deltas (gray, labeled with their initials) are displayed in the same space to probe into the capability of a combined approach of numerical simulations with controlled physical processes and TopoDynamic space projections of simulated and field deltas to refine delta classification and infer process from form (see text for discussion). The dots correspond to the medians of both parameters, i.e., number of alternative paths and Leakage Index, while the vertical and horizontal lines span the corresponding 25th up to the 75th percentiles.

3.2. Inferring Process From Form

Caldwell and Edmonds [2014] showed that delta morphology of river-dominated deltas is sensitive to the dominant grain size and the cohesiveness of the incoming sediment. By visual inspection, the skeletonized deltas in Figure 2 show how the topologic complexity of the channel networks increases as D_{50} increases. We can quantify this observation with the complexity metrics. Indeed, Figure 2 shows that when the sediment grain size increases, the number of alternative paths increases and the Leakage Index decreases.

In Figure 3, we position the simulated deltas in the TopoDynamic complexity space together with the seven field deltas presented in *Tejedor et al*. [2015b]. We first note that a large portion of the TopoDynamic complexity space populated by field deltas can be sampled just by varying the incoming sediment grain size, suggesting that at least in river-dominated deltas and in the absence of other controls (such as vegetation, and flood variability) sediment composition can account to a large degree for the complexity of delta channel network patterns. However, acknowledging the fact that some field deltas can be (1) young in their stages of evolution, (2) shaped by other physical processes (e.g., waves and tides, streamflow variability, and vegetation) in addition to sediment composition, and (3) subject to geologic and other constraints, a close inspection of the TopoDynamic complexity space of Figure 3 in terms of similarities and discrepancies between field and simulated deltas reveals some interesting observations. These observations, discussed below, give confidence for the potential toward building a framework for quantitative delta classification.

1. *Different stage of evolution*: If we compare the river-dominated Wax Lake (W) and Mossy (M) deltas with the deltas generated using Delft3D (also river-dominated) in the TopoDynamic space, it is seen that these two field deltas are bracketed between the simulated deltas with D_{50} in the range of 0.01 and 0.05 mm. These values are significantly lower than the measured field values of $D_{50} = 0.10–0.15$ mm for the Wax Lake and Mossy deltas [*Shaw et al*., 2013; *Caldwell and Edmonds*, 2014]. We propose that this apparent discrepancy might be explained by the different age of the deltas: while the simulated deltas displayed in Figure 3 depict the steady state of fully evolved deltas, both Wax Lake and Mossy deltas are relatively young and still evolving. Based on our preliminary analysis (see Figure 1) these field deltas are expected to reach higher values of N_{ap} and lower values of LI as they grow, approaching their expected positions in the TopoDynamic space consistent with their sediment composition.
2. *Different underlying mechanism*: Some field deltas in Figure 3 are positioned in terms of complexity far from their numerical counterparts with similar sediment composition. An example of this disparity is Niger delta (N), with median sediment size of around 0.15 mm [*Syvitski and Saito*, 2007], which exhibits a higher topologic complexity and lower dynamic complexity than would be expected from the simulated deltas with a similar range of sediment grain size, $D_{50} = 0.10–0.25$ mm (Figure 3). This discrepancy is interpreted as revealing that Niger delta is not river-dominated (as the Delft3D deltas are) pointing out how additional underlying mechanisms such as downstream hydrodynamic boundaries (e.g., waves and tides) might affect network complexity.

3. *Imposed constraints*: We notice that each delta occupies in the TopoDynamic space not only a point but a region defined by the variability in the complexity of the delta subnetworks (whiskers around the solid circles in Figure 3). We posit that valuable information can be extracted from this variability. For example, from Figure 3 it is shown that as D_{50} increases so does the variability (vertical and horizontal whiskers in Figure 3) of both the topologic and dynamic complexity. This is not inconsistent with physical expectation, as coarser sediment has the potential to create more mobile channels and increase avulsion rates resulting in more natural variability among subnetworks as shown for Delft3D simulations [*Caldwell and Edmonds*, 2014]. Therefore, discrepancies between model-predicted and field delta complexity variability might suggest the presence of geologic or human-imposed constraints. For instance, deltas such as Parana (P), which is geologically constrained at its lateral boundaries, is seen to exhibit a reduced degree of variability in the complexity among its subnetworks. Additionally, engineered deltas where the natural mobility of channels is inhibited, together with the proliferation of channelized structures (e.g., ditches and navigable channels) rewiring the connectivity of a delta network can impact significantly the variability in complexity of its subnetworks compared to natural deltas.

Based on the above observations, we propose that a combined approach of controlled simulation (with known drivers) and quantitative comparison of simulated and field deltas, in terms of similarities and differences in their topologic and dynamic complexity, offers a pathway toward systematic understanding of the relation between process and form and eventual delta classification.

4. Conclusions and Future Work

We have examined the control of sediment properties (in the absence of other drivers such as wave and tidal energy, vegetation, and flow variability) on river-dominated delta channel networks and showed that the dominant grain size and sediment cohesiveness leave a clear signature on the topologic structure and the dynamic functioning of a delta at steady state, as captured by two metrics of topologic and dynamic complexity introduced in *Tejedor et al.* [2015b]. Specifically, we showed that increased sediment cohesiveness and smaller-dominant grain size result in channel networks with decreased topologic complexity (smaller number of alternative paths in the apex-to-outlet subnetworks) and increased dynamic complexity (larger flux leakage among apex-to-outlet subnetworks). Furthermore, during delta evolution the topologic complexity increases and dynamic complexity decreases, both reaching almost constant values when the delta has reached a steady state. By plotting field deltas and simulated deltas in a TopoDynamic complexity space we showed encouraging results and provided preliminary evidence toward a path for quantitative delta classification by exploring similarities and discrepancies in the underlying processes and the resulting network complexity. Further progress will require a systematic analysis of a large set of delta patterns generated via numerical or physical (laboratory) modeling, where variables reported in the literature to be major factors on the resulting delta morphology come into play (e.g., flow variability [*Edmonds et al.*, 2010; *Ganti et al.*, 2014; *Canestrelli et al.*, 2014] and relative sea level rise [*Liang et al.*, 2016]). Such analysis, even though it may require the introduction of more dimensions in the TopoDynamic complexity space to enhance its discriminatory power, would allow to construct a comprehensive quantitative phase space of deltas shedding light into the identification of first-order controls from delta form. Additionally, the availability of a larger database of deltas would enable us to explore the emerging pattern observed in the TopoDynamic complexity space, suggesting a characteristic signature of delta channel networks, wherein the number of alternative paths of apex-to-outlet subnetworks (topologic complexity) grows at the expense of reducing the flux leakage of that subnetwork to the rest of the delta (dynamic complexity).

Acknowledgments
Partial support by the FESD Delta Dynamics Collaboratory (NSF grant EAR-1135427) and the Water Sustainability and Climate Program (NSF grant EAR1209402) is gratefully acknowledged. This work is part of the International BF-DELTAS project on "Catalyzing action towards sustainability of deltaic systems" funded by the Belmont Forum (NSF grant EAR-1342944). It is also a tribute to the "Sustainable Deltas 2015" (SD2015) Initiative endorsed by the International Council of Scientific Unions (ICSU), which aims to increase awareness of delta vulnerability worldwide and foster international collaboration, knowledge, and data exchange for actionable research toward delta sustainability. This research benefited from collaborations made possible by NSF grant EAR-1242458 under Science Across Virtual Institutes (SAVI): LIFE (Linked Institutions for Future Earth). A.T. acknowledges financial support from the National Center for Earth-surface Dynamics 2 (NSF grant EAR-1246761) postdoctoral fellowship. We thank Phairot Chatanantavet and John Shaw for their insightful comments, which helped improve the presentation of our work. We also thank the Editor M Bayani Cardenas for an efficient and constructive review process. The data in our article can be provided upon request.

References

Caldwell, R. L., and D. A. Edmonds (2014), The effects of sediment properties on deltaic processes and morphologies: A numerical modeling study, *J. Geophys. Res. Earth Surf.*, *119*, 961–982, doi:10.1002/2013JF002965.

Canestrelli, A., W. Nardin, D. Edmonds, S. Fagherazzi, and R. Slingerland (2014), Importance of frictional effects and jet instability on the morphodynamics of river mouth bars and levees, *J. Geophys. Res. Oceans*, *119*, 509–522, doi:10.1002/2013JC009312.

Edmonds, D., R. Slingerland, J. Best, D. Parsons, and N. Smith (2010), Response of river-dominated delta channel networks to permanent changes in river discharge, *Geophys. Res. Lett.*, *37*, L12404, doi:10.1029/2010GL043269.

Edmonds, D. A., and R. L. Slingerland (2010), Significant effect of sediment cohesion on delta morphology, *Nat. Geosci.*, *3*(2), 105–109, doi:10.1038/ngeo730.

Edmonds, D. A., C. Paola, D. C. J. D. Hoyal, and B. A. Sheets (2011), Quantitative metrics that describe river deltas and their channel networks, *J. Geophys. Res.*, *116*, F04022, doi:10.1029/2010JF001955.

Fagherazzi, S., A. Bortoluzzi, W. E. Dietrich, A. Adami, S. Lanzoni, M. Marani, and A. Rinaldo (1999), Tidal networks: 1. Automatic network extraction and preliminary scaling features from digital terrain maps, *Water Resour. Res.*, *35*(12), 3891–3904, doi:10.1029/1999WR900236.

Galloway, W. E. (1975), Process framework for describing the morphologic and stratigraphic evolution of deltaic depositional systems, in *Deltas: Models for Exploration*, edited by M. L. Broussard, pp. 87–98, Houston Geol. Soc, Houston, Tex.

Ganti, V., Z. Chu, M. P. Lamb, J. A. Nittrouer, and G. Parker (2014), Testing morphodynamic controls on the location and frequency of river avulsions on fans versus deltas: Huanghe (Yellow River), China, *Geophys. Res. Lett.*, *41*, 7882–7890, doi:10.1002/2014GL061918.

Geleynse, N., J. E. A. Storms, D. J. R. Walstra, H. R. A. Jagers, Z. B. Wang, and M. J. F. Stive (2011), Controls on river delta formation: Insights from numerical modelling, *Earth Planet. Sci. Lett.*, *302*(1–2), 217–226, doi:10.1016/j.epsL2010.12.013.

Hiatt, M., and P. Passalacqua (2015), Hydrological connectivity in river deltas: The first-order importance of channel-island exchange, *Water Resour. Res.*, *51*, 2264–2282, doi:10.1002/2014WR016149.

Hoyal, D. C. J. D., and B. A. Sheets (2009), Morphodynamic evolution of experimental cohesive deltas, *J. Geophys. Res.*, *114*, F02009, doi:10.1029/2007JF000882.

Jerolmack, D. J., and J. B. Swenson (2007), Scaling relationships and evolution of distributary networks on wave-influenced deltas, *Geophys. Res. Lett.*, *34*, L23402, doi:10.1029/2007GL031823.

Lam, L., S.-W. Lee, and C. Y. Suen (1992), Thinning methodologies—A comprehensive survey, *IEEE Trans. Pattern Anal. Mach. Intell.*, *14*(9), 869–885.

Lesser, G. R., J. A. Roelvink, J. A. T. M. van Kester, and G. S. Stelling (2004), Development and validation of a three-dimensional morphological model, *Coast. Eng.*, *51*(8–9), 883–915, doi:10.1016/j.coastaleng.2004.07.014.

Liang, M., V. R. Voller, and C. Paola (2015a), A reduced-complexity model for river delta formation: Part 1—Modeling deltas with channel dynamics, *Earth Surf. Dyn.*, *3*, 67–86, doi:10.5194/esurf-3-67-2015.

Liang, M., N. Geleynse, D. A. Edmonds, and P. Passalacqua (2015b), A reduced-complexity model for river delta formation: Part 2—Assessment of the flow routing scheme, *Earth Surf. Dyn.*, *3*, 87–104, doi:10.5194/esurf-3-87-2015.

Liang, M., C. Van Dyk, and P. Passalacqua (2016), Quantifying the patterns and dynamics of river deltas under conditions of steady forcing and relative sea-level rise, *J. Geophys. Res. Earth Surf.*, *121*, 465–496, doi:10.1002/2015JF003653.

Marra, W. A., M. G. Kleinhans, and E. A. Addink (2014), Network concepts to describe channel importance and change in multichannel systems: Test results for the Jamuna River, Bangladesh, *Earth Surf. Processes Landforms*, *39*, 766–778.

Morisawa, M. (1985), Topologic properties of delta distributary networks, in *Models in Geomorphology*, edited by M. J. Woldenberg, pp. 239–268, Allen and Unwin, St. Leonards, NSW, Australia.

Nienhuis, J. H., A. D. Ashton, and L. Giosan (2015), What makes a delta wave-dominated?, *Geology*, doi:10.1130/G36518.1.

Orton, G. J., and H. G. Reading (1993), Variability of deltaic processes in terms of sediment supply, with particular emphasis on grain size, *Sedimentology*, *40*, 475–512, doi:10.1111/j.1365-3091.1993.tb01347.x.

Passalacqua, P., S. Lanzoni, C. Paola, and A. Rinaldo (2013), Geomorphic signatures of deltaic processes and vegetation: The Ganges-Brahmaputra-Jamuna case study, *J. Geophys. Res. Earth Surf.*, *118*, 1838–1849, doi:10.1002/jgrf.20128.

Rinaldo, A., S. Fagherazzi, S. Lanzoni, M. Marani, and W. E. Dietrich (1999a), Tidal networks: 2. Watershed delineation and comparative network morphology, *Water Resour. Res.*, *35*(12), 3905–3917, doi:10.1029/1999WR900237.

Rinaldo, A., S. Fagherazzi, S. Lanzoni, M. Marani, and W. E. Dietrich (1999b), Tidal networks: 3. Landscape-forming discharges and studies in empirical geomorphic relationships, *Water Resour. Res.*, *35*(12), 3919–3929, doi:10.1029/1999WR900238.

Shaw, J. B., M. A. Wolinsky, C. Paola, and V. R. Voller (2008), An image-based method for shoreline mapping on complex coasts, *Geophys. Res. Lett.*, *35*, L12405, doi:10.1029/2008GL033963.

Shaw, J. B., D. Mohrig, and S. K. Whitman (2013), The morphology and evolution of channels on the Wax Lake Delta, Louisiana, USA, *J. Geophys. Res. Earth Surf.*, *118*, 1562–1584, doi:10.1002/jgrf.20123.

Smart, J. S., and V. L. Moruzzi (1971), Quantitative properties of delta channel networks, Technical Report #3, 27 pp., IBM Thomas J. Watson Research Center, Yorktown Heights, New York.

Straub, K. M., Q. Li, and W. M. Benson (2015), Influence of sediment cohesion on deltaic shoreline dynamics and bulk sediment retention: A laboratory study, *Geophys. Res. Lett.*, *42*, 9808–9815, doi:10.1002/2015GL066131.

Syvitski, J. P. M., and Y. Saito (2007), Morphodynamics of deltas under the influence of humans, *Global Planet. Change*, *57*, 261–282, doi:10.1016/j.gloplacha.2006.12.001.

Tejedor, A., A. Longjas, I. Zaliapin, and E. Foufoula-Georgiou (2015a), Delta channel networks: 1. A graph-theoretic approach for studying connectivity and steady state transport on deltaic surfaces, *Water Resour. Res.*, *51*, 3998–4018, doi:10.1002/2014WR016577.

Tejedor, A., A. Longjas, I. Zaliapin, and E. Foufoula-Georgiou (2015b), Delta channel networks: 2. Metrics of topologic and dynamic complexity for delta comparison, physical inference, and vulnerability assessment, *Water Resour. Res.*, *51*, 4019–4045, doi:10.1002/2014WR016604.

Van Rijn, L. C. (1984a), Sediment transport; Part I, Bed load transport, *J. Hydraul. Eng.*, *110*(10), 1431-1456.

Van Rijn, L. C. (1984b), Sediment transport; Part II, Suspended load transport, *J. Hydraul. Eng.*, *110*(11), 1613–1641.

Wolinsky, M. A., D. A. Edmonds, J. Martin, and C. Paola (2010), Delta allometry: Growth laws for river deltas, *Geophys. Res. Lett.*, *37*, L21403, doi:10.1029/2010GL044592.

Wright, L. D., and J. M. Coleman (1973), Variations in morphology of major river deltas as functions of ocean wave and river discharge regimes, *AAPG Bull.*, *57*(2), 370–398.